The role of subgrain boundaries in partial melting

Jamie S.F. Levine [a, *], Sharon Mosher [a], Jeffrey M. Rahl [b]

[a] Department of Geological Sciences, Jackson School of Geosciences, University of Texas at Austin, Austin, TX, 78712, USA
[b] Department of Geology, Washington and Lee University, Lexington, VA, 24450, USA

A R T I C L E   I N F O

A B S T R A C T

Evidence for partial melting along subgrain boundaries in quartz and plagioclase is documented for rocks from the Lost Creek Gneiss of the Llano Uplift, central Texas, the Wet Mountains of central Colorado, and the Albany-Fraser Orogen, southwestern Australia. Domains of quartz or plagioclase crystals along subgrain boundaries are preferentially involved in partial melting over unstrained domains of these minerals. Material along subgrain boundaries in quartz and plagioclase has the same morphology as melt pseudomorphs present along grain boundaries and is commonly laterally continuous with this former grain boundary melt, indicating the material along subgrain boundaries can also be categorized as a melt pseudomorph. Subgrain boundaries consist of arrays of dislocations within a crystal lattice, and unlike fractures would not act as conduits for melt migration. Instead, the presence of former melt along subgrain boundaries requires that partial melting occurred in these locations because it is kinetically more favorable for melting reactions to occur there. Preferential melting in high strain locations may be attributed to strain energy, which provides a minor energetic contribution to the reaction and leads to preferential melting in locations with weakened bonds, and/or the presence of small quantities of water associated with dislocations, which may enhance diffusion rates or locally lower the temperature needed for partial melting.

1. Introduction

In the last 40 years, great strides have been made in understanding the role of strain in promoting metamorphic reactions. Internal plastic strain of crystal lattices induces dislocations which may form tangles or migrate to form walls of dislocations, depending primarily on the rate of diffusion relative to the rate of strain. With increased strain and/or temperature, dynamic recrystallization may occur 1) through subgrain rotation recrystallization as walls of dislocations transition from subgrain to discrete grain boundaries as a result of further migration of dislocations into walls, or 2) through migration of grain boundaries of less strained grains into more strained grains (Urai et al., 1986). Both of these processes lower the stored lattice strain energy and lead to formation of new strain-free grains with most remaining dislocations at the grain boundaries (Poirier, 1985). A decrease in grain size caused by dynamic recrystallization at highly strained locations leads to increased rates of diffusion, as well as more surface area for

reactions to occur, and associated increases in reaction rates (Wintsch, 1975; White, 1975; Kerrich et al., 1977; Brodie and Rutter, 1985; Yund and Tullis, 1991).

Highly strained locations commonly have faster reaction rates, due to increased dislocation density, finer grain size, and enhanced diffusion rates; the latter has been attributed to pipe diffusion along linear dislocation arrays (Smoluchowski, 1952; Luther, 1965; Etheridge et al., 1984; Yurimoto and Nagasawa, 1989; Piazolo et al., 2016). Dislocations commonly have water bonded to the crystal lattice, visible in the transmission electron microscope (TEM) as water bubbles located at dislocations, which enhances diffusion rates (Green and Radcliffe, 1975; McLaren et al., 1983; Kronenberg et al., 1986, 1990; Meng et al., 2009). Strain solution, a process of preferential dissolution in higher strain locations, may increase chemical potential gradients of dissolved species and associated reaction rates (Wintsch and Dunning, 1985).

Partial melting reactions typically occur along interfaces or surfaces, such as grain boundaries, because interfaces are locations where reactant minerals are in contact with each other. In many cases water or other fluids, which enhance melting rates, are found along grain boundaries and are associated with the dislocations organized into high density arrays such as subgrain boundaries.

* Corresponding author. Department of Geology, Appalachian State University, Boone, NC, 28608, USA.
E-mail address: levinejs@appstate.edu (J.S.F. Levine).

Subgrain boundaries are recovery features with lower dislocation densities than the interior of deformed crystals, but importantly can be connected to the grain boundaries, interfaces along which melting reactions commonly take place.

In this study we investigate the role of strain in preferentially inducing melting in locations of high dislocation density, specifically along subgrain boundaries in quartz and plagioclase grains. Below we give background on the role of strain and dislocations in melting and briefly discuss melt microstructures attributed to identification of former melt. We also provide evidence of melting along subgrain boundaries in quartz and plagioclase from three different field areas, and discuss possible mechanisms for partial melting in these locations.

2. The melting process and the role of strain

Within the material science, physics, and metallurgical communities, studies of melting in monomineralic substances or even single crystals have shown that melting occurs along grain boundaries or surfaces (Dash, 1999 and references therein; Alsayed et al., 2005; Mei and Lu, 2007 and references therein; Han et al., 2010), and in one component systems melting preferentially occurs at high strain locations (Lutsko et al., 1989; Tartaglino and Tosatti, 2003; Alsayed et al., 2005; Sirong et al., 2006; Han et al., 2010), as a simple transformation of solid to liquid. Theoretical calculations have suggested that melting preferentially occurs in areas with high defect density, including dislocations, stacking faults, vacancies, and impurities (Mott, 1952; Mizushima, 1960; Ookawa, 1960; Kuhlmann-Wilsdorf, 1965).

Many studies have specifically investigated premelting, a process in which melting begins below the thermodynamically calculated melting temperature (Pluis et al., 1987; Mei and Lu, 2007 and references therein). Several premelting studies focused both on interfaces and defects by examining the role of strain in preferential melting along grain boundaries, subgrain boundaries, or strained surfaces (Tartaglino and Tosatti, 2003; Alsayed et al., 2005; Han et al., 2010). Alsayed et al. (2005) documented premelting in colloidal silica gels preferentially located along grain boundaries, or along partial dislocations in regions that did not contain or were far from grain boundaries. Metals and geologic materials have much higher melting temperatures than colloidal silica gels, and conducting in-situ observational experiments on melting of these substances is difficult. Instead, molecular dynamics simulations provide a tool for analyzing the role of strain on the melting process in materials with high melting temperatures. One molecular dynamics simulation evaluated differences in surface melting between strained and unstrained Al (Tartaglino and Tosatti, 2003), whereas another compared melting of Cu at a low and a high energy grain boundary (Han et al., 2010). In both studies, more highly strained and higher energy locations melted at lower temperatures than unstrained or lower energy regions. Together, these studies (Tartaglino and Tosatti, 2003; Alsayed et al., 2005; Han et al., 2010) provide compelling evidence that more highly strained regions preferentially undergo melting.

The geological community however, has not focused on the role of strain in partial melting, except in a few cases. Hand and Dirks (1992) proposed that melting preferentially occurred in crenulated regions of the Napperby Gneiss, northern Australia because of increased stored strain energy, surface free energy, and smaller grain size. An experimental study on melting in strained metapelites concluded that more melting occurred in more highly strained locations, possibly caused by smaller grain size, shear heating, or chemical or thermal effects from changes in mean stress during melting (Misra et al., 2009). A follow-up study supported these findings, but indicated that the exact role that deformation plays remains unknown (Tumarkina et al., 2011). Finally, Seaman et al. (2013) have suggested that deformation plays a role in moving small quantities of water, associated with defects or fluid inclusions, from the interior of nominally-anhydrous minerals, to grain boundaries, where relict films of partial melt are located. Together these studies suggest an important role for deformation in promoting partial melting, even as the mechanism is not yet understood.

3. Geologic settings

Samples for this study were taken from three field areas: the Llano Uplift of central Texas, the Wet Mountains of central Colorado, and the Albany-Fraser Belt of southwestern Australia. All three locations contain Mesoproterozoic-aged rocks with evidence for partial melting and were chosen primarily because they had sufficiently low melt contents to preserve melt microstructures. Additionally, minimal subsequent tectonism in each setting prevented the destruction of these delicate melt microstructures by post-melting deformation.

Identifying the reactions that have occurred in each location is fundamental for understanding where melting occurred within the rock. Granitic gneisses of the Lost Creek Gneiss in the western Llano Uplift experienced granite wet melting (see Levine and Mosher, 2010 for a description of melting reactions) at conditions of approximately 700 °C and 0.7 GPa (Carlson et al., 2007). Melting in the Wet Mountains occurred through dominantly biotite-dehydration and granite wet melting, with rare muscovite-dehydration reactions (see Levine et al., 2013 for a complete description of melting reactions). Rocks have a range of compositions, but granitic and metapelitic gneisses provide the best evidence for partial melting and indicate peak temperatures in the range of 650–800 °C with moderate pressures (Siddoway et al., 2000; Levine et al., 2013). Albany-Fraser Belt melting occurred primarily through fluid-present and -absent biotite- and amphibole-dehydration melting and conditions were at least 800–850 °C and 0.7–0.8 GPa (Bodorkos and Clark, 2004; Levine, 2011), but pegmatites formed during late-stage deformation record temperatures of 800–1000 °C (Black et al., 1992). The most common rock types are quartz monzonitic, quartz dioritic, granodioritic, and tonalitic orthogneisses. Despite differences in lithologies and melting reactions in these three diverse locations, thin sections from each location preserve textures attributed to the former presence of melt.

4. Methods

4.1. Criteria for recognizing former melt in thin section

The presence of former melt in thin section is inferred from textural relationships between reactant minerals and characteristic shapes and spatial locations of minerals interpreted to have formed from former melt. In areas that have undergone granitic wet melting, the presence of small blebs of material along unlike grain boundaries, serrate and cuspate grain boundaries with low dihedral angles between former melt and adjacent minerals, and the string-of-beads texture, with small blebs of minerals that came from former melt of different compositions along grain boundaries, are all characteristic of melt pseudomorphs (Harte et al., 1991; Sawyer, 1999, 2001; Rosenberg and Riller, 2000; Holness and Isherwood, 2003; Holness and Sawyer, 2008; Holness et al., 2011; Levine et al., 2013). Rocks that have undergone dehydration melting typically display corroded and skeletal reactant minerals, associated with crystallization products from films of former melt adjacent to these grains, and peritectic products of melting, typically

with euhedral crystal faces, surrounded by an envelope of material that represents former melt (Sawyer, 1999, 2001; Waters, 2001; Barbey, 2007; Holness and Sawyer, 2008; Levine et al., 2013).

In rocks that have experienced granitic wet melting, the melt produced from partial melting is made up of K-feldspar, plagioclase, and quartz components. As the melt begins to crystallize, the various components of the melt nucleate onto preexisting grains of like composition (Harte et al., 1991; Rosenberg and Riller, 2000; Holness and Sawyer, 2008). For example, if melt is located between grains of quartz and plagioclase, but there is no K-feldspar present because it was completely consumed during melting, the quartz component of the melt will nucleate onto the quartz grains, the plagioclase component of the melt will nucleate onto plagioclase grains, and the remaining melt will crystallize as a new grain of K-feldspar because there were not any preexisting grains of K-feldspar on which to nucleate. Consequently, melt pseudomorphs are composed of the least abundant phase in the melting reaction.

Previous workers have not described the presence of melt pseudomorphs along subgrain boundaries. However, blebs of material along subgrain boundaries that have a similar morphology and texture to melt pseudomorphs along grain boundaries with serrate/cuspate grain boundaries and low solid-solid dihedral angles are observed, and are inferred to be former melt (Levine et al., 2013; this study). Additionally, the material that is inferred to be former melt along subgrain boundaries maintains optical continuity with, and/or is connected to, former melt along the adjacent grain boundary. Consequently, we propose that the presence of blebs of material along subgrain boundaries with a different composition than the host mineral, and low solid-solid and solid-melt dihedral angles is a new microstructure indicative of former melt.

4.2. Criteria for identifying subgrain boundaries

4.2.1. Optical microscopy

Subgrain boundaries can be identified optically in thin section, under crossed-polars, by a sharp change in extinction across a boundary not associated with a fracture within a larger grain. In plane-polarized light, the subgrain boundary is not visible. Fractures are visible in both crossed- and plane-polarized light, however, and a change in extinction may be observed. Changes in extinction in crossed-polarized light associated with fluid inclusions in plane-polarized light likely represent healed fractures and not subgrain boundaries.

4.2.2. Electron backscatter diffraction

In quartz, mineral extinction in crossed-polarized light varies only with the orientation of the *c*-axis (McLaren et al., 1970; Trépied et al., 1980). In contrast, the electron backscatter diffraction (EBSD) technique provides a more complete description of the crystallographic orientation of quartz (e.g., Prior et al., 1999), allowing for a robust identification of subgrain boundaries and their associated crystallographic misorientations (Lloyd et al., 1997). The misorientation between subgrain boundaries can be characterized by a single rotation along a particular rotation axis (Lloyd et al., 1997). Although several axis/angle pairs may be consistent with a given misorientation, the axis with a minimum misorientation angle is typically selected (Mainprice et al., 1993; Lloyd et al., 1997).

Relating the crystallographic misorientations around subgrain boundaries to slip systems active during deformation provides strong evidence that the optically-identified boundaries are true subgrain walls rather than other features such as microcracks. Recognizing the slip system associated with a subgrain boundary involves identifying the rotation associated with slip. Two approaches that have proven useful are 1) mapping "rotation trajectories" from observations near a subgrain boundary to reveal a pole of rotation on a pole figure, or 2) plotting misorientation axes on an inverse pole figure to reveal the crystallographic axis of rotation (Lloyd et al., 1997; Neumann, 2000; Menegon et al., 2011). In quartz, the activity of the various slip systems varies with temperature, and thus this type of analysis provides insight into the deformation conditions (Kruhl, 1998; Morgan and Law, 2004).

Crystallographic orientations of selected grains were measured using an EVO MA 15, Scanning Electron Microscope (SEM) at Washington and Lee University using an Oxford Instruments EBSD detector and Aztec software. Standard mechanically-polished thin sections were prepared for EBSD analysis with a final chemical-mechanical polishing step using a 0.04 μm colloidal silica slurry. Analytical conditions were an accelerating voltage of 25 kV, a probe current of 15–20 nA, a working distance of about 22 mm, and a 70° sample tilt. Samples were uncoated, so low-vacuum conditions (30 Pa) were used to prevent charging. Quartz in the areas described below was mapped on a two-dimensional rectangular grid with a step size of 2 μm.

EBSD data were processed using the MTEX toolbox for Matlab (Hielscher and Schaeben, 2008). Within mapped areas, quartz grains were identified using a 10° threshold (White, 1977), using the MTEX grain identification algorithm (Bachmann et al., 2011). Data are presented below in lower hemisphere pole figures, misorientation transects, and inverse pole figures of misorientation axes between subgrains. Misorientation axes can be readily calculated from EBSD observations, but there may be large errors particularly when the misorientation angle between the grains is low (i.e., <10°) (Prior, 1999). Nevertheless, the misorientation axes described below are consistent with activity on common slip systems within quartz.

5. Microstructures and petrography

5.1. Lost Creek Gneiss, Llano Uplift samples

Samples from the Lost Creek Gneiss, central Texas, provide evidence for partial melting during very latest deformation, and melting likely continued after deformation had ceased. Melt pseudomorphs are interpreted in these rocks on the basis of the abundance of serrate/cuspate grain boundaries and films of interpreted former melt between unlike phases on grain boundaries. Subgrain boundaries in quartz and plagioclase were identified optically on the basis of sharp changes in extinction, and the presence of these boundaries in quartz was confirmed by measurements of crystallographic orientation using EBSD (Figs. 1–3).

Within these rocks, melt pseudomorphs preserved on subgrain boundaries in both quartz and plagioclase (Fig. 1) are interpreted based on their textural similarities and lateral continuity with melt pseudomorphs on grain boundaries. Most of the former melt in Lost Creek Gneiss samples is now preserved as K-feldspar, and equal abundances of former melt occur along subgrain boundaries in quartz and plagioclase. Many of the coarse quartz grains display chessboard extinction, which has two orthogonal subgrain orientations resulting from synchronous activity of prism[c] and basal<a> slip (Kruhl, 1996). Blebs of K-feldspar are commonly located along only one of the subgrain orientations within these quartz grains (Fig. 1A and B). In a few cases, former melt follows both orientations, and the melt pseudomorph forms a diamond shape with curved boundaries and cuspate morphologies (Fig. 1A). Former melt is typically found along the part of the subgrain that intersects the grain boundary, which may also contain former melt (Fig. 1A and B). Melt pseudomorphs within quartz are as wide as 100 μm across and extend along the subgrain boundary for up to 1 mm (Fig. 1A and B). These films of former melt typically end in a
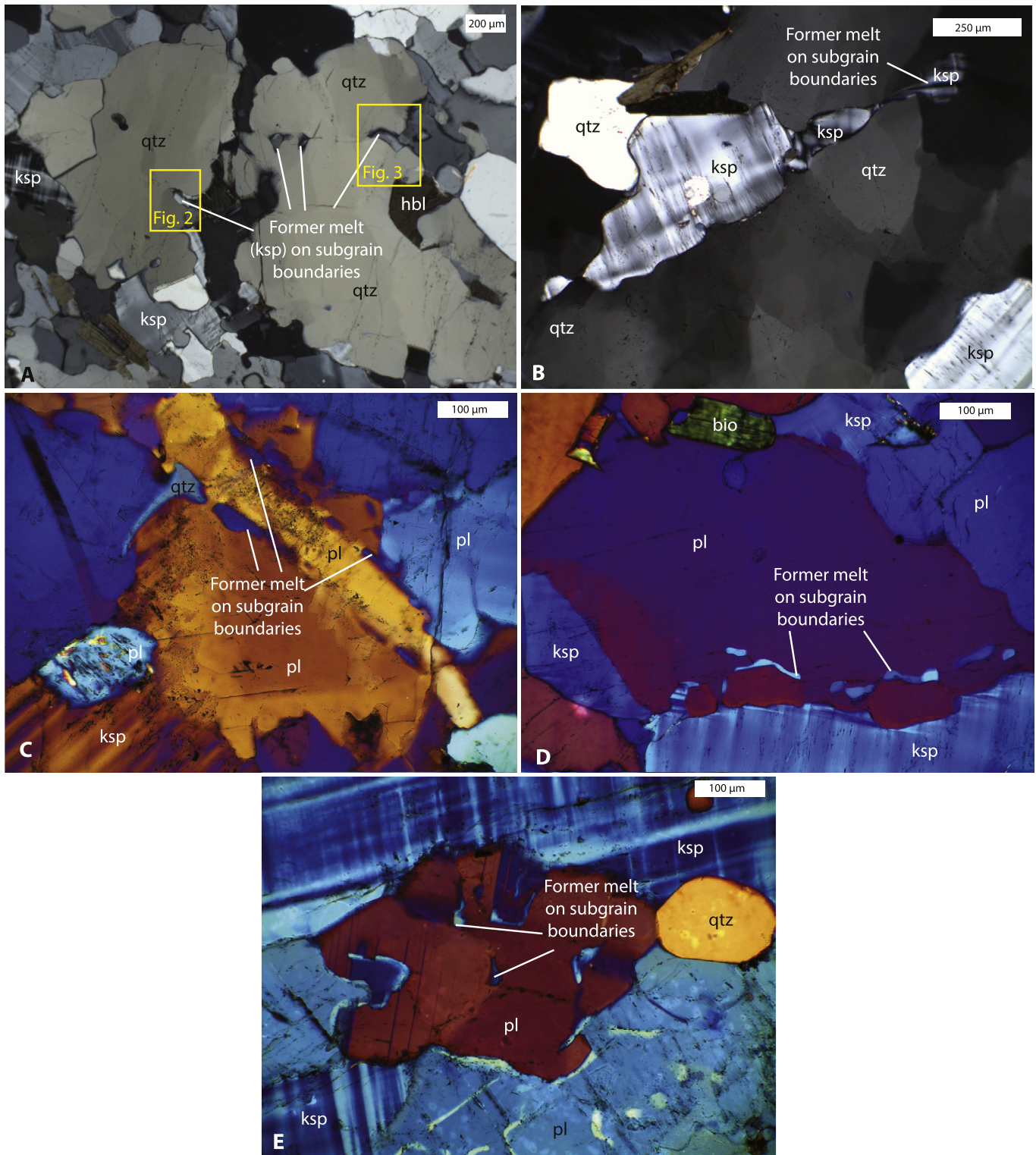
Fig. 1. Photomicrographs of former melt along subgrain boundaries in rocks from the Lost Creek Gneiss, of the Llano Uplift, central Texas. All images taken in crossed polars; all but A & B with gypsum plate. A. Former melt, now K-feldspar, on subgrain boundaries in quartz. Former melt is found along the edge of the subgrain boundary near the grain boundary, and there are also isolated blebs of former melt within the interior of the quartz grain along the subgrain boundary. All of the former melt has a cuspate shape and is 50–75 μm in width. Yellow boxes marked Figs. 2 and 3 are locations of EBSD misorientation maps shown in Figs. 2 and 3 respectively. B. Former melt, now K-feldspar (displays microcline twinning), along subgrain boundary in quartz. Former melt is connected to a larger melt pseudomorph along the grain boundary. The former melt along the subgrain boundary has a rounded tip and variable thickness, up to 100 μm, along its length. C. Former melt (blue), now quartz, along subgrain boundary in plagioclase (orange). This melt pseudomorph is mostly discontinuous and is seen as blebs along two parallel subgrain boundaries. These blebs have rounded tips and are 10–30 μm in width. D. Former melt (blue), now K-feldspar, along subgrain boundaries in plagioclase (purple). This melt pseudomorph is discontinuous, with rounded tips and is less than 20 μm in width. E. Melt pseudomorph (blue), now quartz, along subgrain boundaries in plagioclase (pink). Former melt forms discontinuous blebs, is 10–20 μm in width, and is found primarily in the interior of the grain. qtz = quartz, ksp = K-feldspar, pl = plagioclase, and hbl = hornblende.
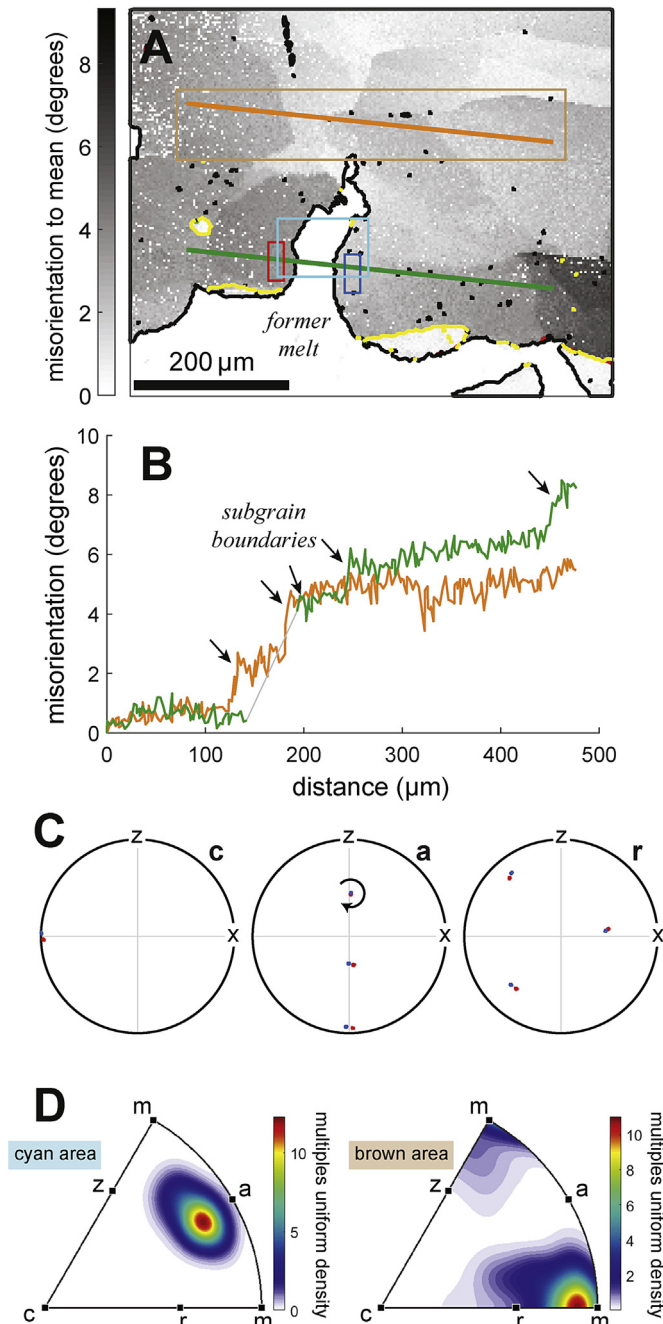
Fig. 2. A. Processed quartz EBSD map showing the misorientation angle of each pixel relative to the mean orientation of its grain, highlighting the low-angle subgrain structure. See Fig. 1A for location. A finger of former melt is oriented vertically, parallel to the basal plane of the quartz crystal. Yellow lines separate regions with misorientations of 60° around the c-axis, interpreted as Dauphiné twins. Red lines separate regions with misorientations of 2–10°. The position of the misorientation transects shown in B are indicated by the orange and green lines; data from the red and blue areas are plotted in the pole figures shown in C; misorientation axes created from pixels enclosed in the cyan and brown boxes are shown in D. B. Profiles showing the misorientation of each point along the transects in A are measured relative to the initial point. The data show domains of consistent orientation separated by steps interpreted as subgrain boundaries. The step across former melt in the green profile is shown by a thin gray line. C. Pole figures showing the (c), {a}, and {r} directions from the blue and red areas shown in A. No distinction is drawn between the positive and negative {a} directions. The data suggest rotation around the a-axis across the former melt finger. D. Contour plot of misorientation axes with misorientation angles between 2 and 10° between pixels. Data come from within the cyan and brown areas shown in A, suggesting misorientation around {a} and {m}, respectively.

point and are cuspate-shaped (Fig. 1A), but rare examples show a less angular shape and a rounded tip (Fig. 1B).

Plagioclase grains typically have melt pseudomorphs along several parallel subgrain boundaries (Fig. 1C and D) or along subgrain boundaries in multiple orientations within the same grain (Fig. 1E), locally outlining most of the subgrain (Fig. 1D). In many cases melt pseudomorphs are discontinuous blebs of former melt along an individual subgrain boundary (Fig. 1C and D). These blebs of former melt are 10–30 μm wide and are 100–200 μm long; they display only minor variations in thickness along the length of the melt pseudomorph. Many of these melt pseudomorphs have rounded or square tips (Fig. 1C and D), although rare blebs have pointed tips (Fig. 1E). Within plagioclase grains it is usually difficult to determine the composition of the melt pseudomorph because the blebs of former melt are fine-grained.

Two of the subgrain boundaries in Fig. 1A were further characterized by EBSD analysis (Figs. 2 and 3). Grain boundaries with a misorientation around the quartz c-axis of 60 ± 1° were identified (marked with yellow lines in Fig. 2A). These represent Dauphiné twins, in which a 180° rotation around the quartz c-axis in quartz switches the position of the {r} and {z} planes (Frondel, 1962; Tullis and Tullis, 1972). Within each grain or Dauphiné twin, the misorientation of each pixel relative to the mean orientation of that domain was calculated (Fig. 2A). The resulting misorientation map of quartz highlights regions of similar orientation separated along sharp boundaries from other regions of nearly uniform orientation. To visualize the degree of misorientation, we present misorientation transects across the grain (Fig. 2A, B), including areas unaffected (orange transect) and affected (green transect) by partial melting. The transects show the degree of misorientation of each pixel relative to the initial point on the transect. Both transects show regions of consistent orientation separated by narrow zones (i.e., subgrain boundaries) across which there are distinct changes in orientation. Both the map and transects demonstrate that the misorientation between subgrains is typically low (between 1.0 and 2.0°), but at values within the resolution of the EBSD technique (Humphreys et al., 1999; Pennock and Drury, 2005). The observed noise within the data is generally less than 0.5°, as evidenced by the oscillations around a consistent value within regions of similar orientation. This variation is less than the misorientation between the domains, further validating resolution of subgrains with misorientations as low as 1.0–2.0°. Notably, the misorientation across the former melt film (green transect) is larger, approximately 4°.

The EBSD data show that the quartz c-axis is oriented E-W in the image (Fig. 2A), perpendicular to the finger of former melt, indicating that melting occurred parallel to the basal plane of quartz. To visualize the crystallographic orientations across the region of former melt, we have plotted crystallographic preferred orientation measurements from either side of the former melt finger (red and blue boxes in Fig. 2A) (Fig. 2C). These pole figures show similar orientations, but with a small but apparent rotation around one of the a-axes. This sense of rotation is further illustrated by an inverse pole figure of misorientation axes calculated by comparing the misorientations between 2 and 10° between pixels within the cyan box (Fig. 2D). This shows a maximum for misorientation near the a-axis (Fig. 2D), which is associated with the prism[c] slip system, assuming the subgrain wall represents a tilt boundary (Lloyd et al., 1997; Neumann, 2000). A similar analysis of the orange transect area (brown box) shows a dominant misorientation axis around {m}, consistent with activity of the basal<a> system (Mainprice et al., 1993; Lloyd et al., 1997; Neumann, 2000). This pairing of active slip systems is consistent with the development of chessboard extinction, which is characteristic of deformation at high temperatures and/or wet conditions (Mainprice et al., 1986; Okudaira et al., 1995; Kruhl, 1996).
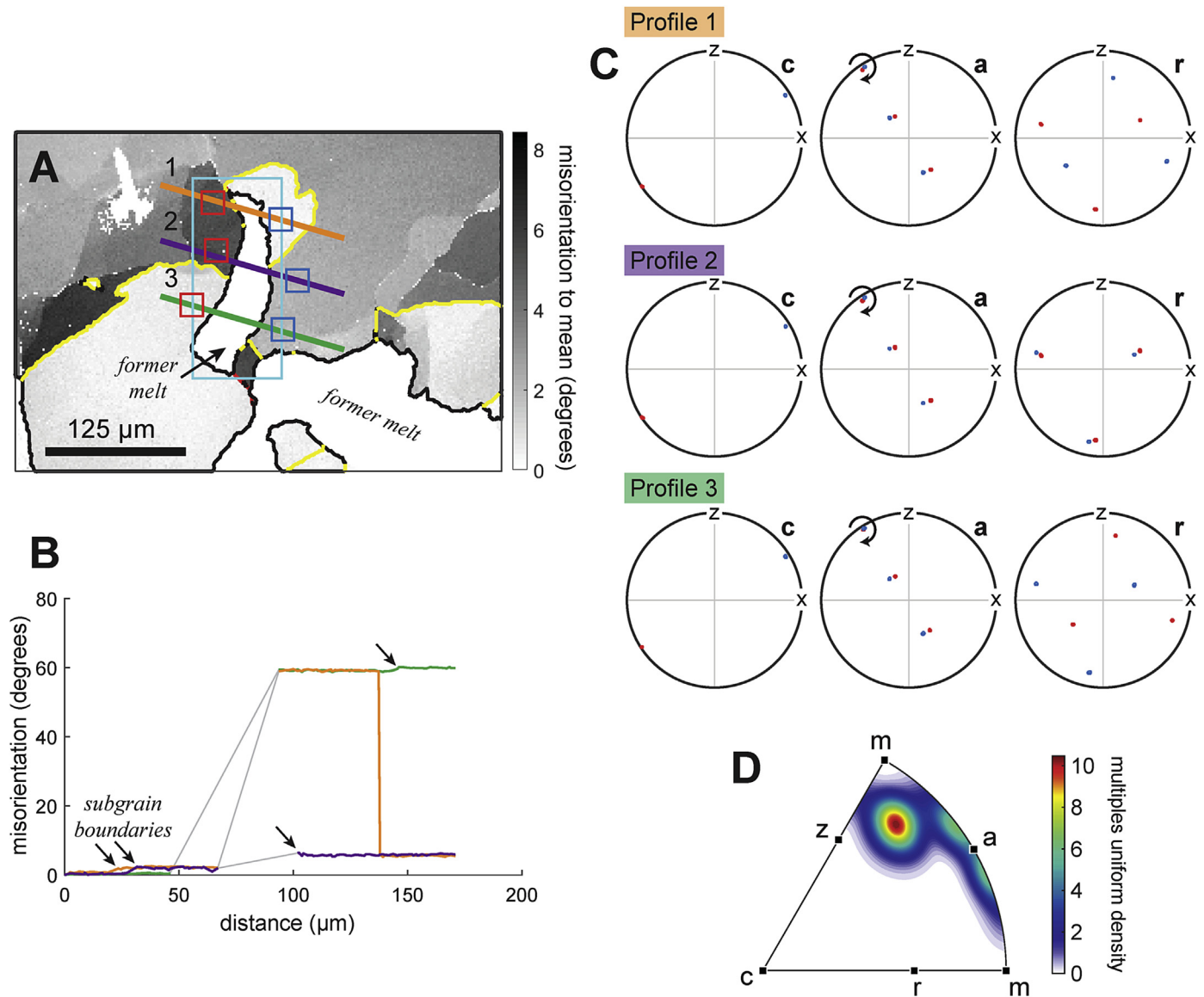
Fig. 3. Quartz EBSD data for area shown in Fig. 1A; plotting conventions are the same as those in Fig. 2. A. Misorientation map, showing both a subgrain boundary and Dauphiné twins near the former melt bleb. B. Misorientation profile, showing subgrains within all three transects and nearly 60° misorientation steps across the former melt bleb along the orange and green transects. C. Pole figures illustrating rotation around the quartz *a*-axis across the melt bleb for all three transects; Dauphiné twinning along the orange and green transects is illustrated by the {r} pole figures that show 60° rotation despite similar *c* and *a*-axes. D. Misorientation axes from the cyan area, indicating rotation around *a* as well as another axis positioned between {z}, {m}, and {a}.

EBSD misorientation data is also provided for the box in Fig. 1A that is marked Fig. 3, with data plotted using the same conventions described for Fig. 2. This misorientation map shows three transects which cross a bleb of former melt (Fig. 3A). The purple transect shows three distinct changes in misorientation (Fig. 3A) which correspond to subgrain boundaries with orientation changes of approximately 2° in the first step (at approximately 30 μm from the left side of the transect), and 3—4° across the former melt bleb (Fig. 3B). The orange and green transects notably show an approximately 60° misorientation across the former melt bleb (Fig. 3B). The pole figures (Fig. 3C) from the red and blue areas shown along profiles 1 and 3 show similar *c*-axis and *a*-axis orientations but the positions for the {r} planes differ by 60°, indicating the presence of Dauphiné twins across the former melt film (Fig. 3A). Misorientation axes calculated from the region around the former melt bleb (the cyan box in Fig. 3A) show rotation around the

quartz *a*-axis (Fig. 3D), consistent with data from the blue and red areas shown on the pole figures (Fig. 3C), again suggesting activity of the prism[c] slip system. The inverse pole figure shows a significant rotation axis nearly equidistant from {m}, {z}, and {a} (Fig. 3D). This may indicate the presence of twist boundaries, although Neumann (2000) notes that a tilt boundary that develops from the {z}⟨a+c⟩ system will have a rotation axis near this location.

The common occurrence of Dauphiné twins near the subgrain boundaries with former melt, as well as twin boundaries that contain former melt, raises questions about their association. Dauphiné twinning is increasingly recognized within deformed quartz-bearing rocks (e.g., Lloyd, 2004; Pehl and Wenk, 2005; Menegon et al., 2011), and at least three mechanisms for twin formation have been identified: reorientation of the crystal lattice 1) in response to stress to align the more compliant direction

parallel to the maximum compressive stress (Tullis and Tullis, 1972; Menegon et al., 2011); 2) during phase transformation from β-quartz (hexagonal) to α-quartz (trigonal) associated with cooling from the high-to low-temperature stability fields (Nord, 1994; Wenk et al., 2009); or 3) during grain growth by grain boundary migration (Piazolo et al., 2005). Although peak metamorphic conditions were within the stability field for β-quartz, consistent with observations of chessboard extinction which occurs at high (>650 °C) temperatures (Kruhl, 1996), a phase transformation origin upon cooling for the twins seems unlikely. This mechanism should result in the extensive development of twins throughout the sample (see Wenk et al., 2009), whereas the observed Dauphiné twins are heterogeneously developed (cf. Figs. 2 and 3). The variable nature of these twins is suggestive of a stress-induced origin that preferentially impacted grains well-oriented for twinning, perhaps further accentuated by grain growth (e.g., Piazolo et al., 2005). Additionally, some of the twin boundaries contain former melt, which formed at temperatures within the β-quartz stability field, precluding those twins from forming as a result of the later phase transition. These twins are most likely relicts from deformation on the prograde path; Wenk et al. (2009) have shown that bulk rock CPO textures, including Dauphiné twins, can be "remembered" through a transition into and back out of the β-quartz stability field. Although it is possible for twins to represent a response to stresses experienced during retrogression, presence of former melt along some twin boundaries requires those to be present at high temperatures, and the undistorted nature of the former melt blebs suggest a minimal amount of post-melting strain.

Former melt microstructures at grain boundaries within the Lost Creek Gneiss rocks are morphologically similar to the former melt microstructures along subgrain boundaries. Melt pseudomorphs along grain boundaries are 10—100 μm in width and may only extend for several hundred μm; thus the melt may not have wetted the entire grain boundary between two minerals. At triple or quadruple junctions there are larger regions of former melt, up to 500 μm in width, with cuspate edges, similar in morphology to melt pools described by Seaman et al. (2013).

5.2. Wet mountains, central Colorado

Samples from the Wet Mountains provide evidence for syndeformational partial melting. Melt pseudomorphs are interpreted in these rocks using criteria identified by previous workers (Harte et al., 1991; Sawyer, 1999; Rosenberg and Riller, 2000; Holness and Sawyer, 2008), including: serrate and cuspate grain boundaries with low dihedral angles between inferred former melt and adjacent minerals, thin melt pseudomorphs along unlike grain boundaries, and skeletal or corroded reactant minerals. Subgrains in quartz and plagioclase were identified optically based on sharp changes in extinction and subgrain boundaries in quartz were confirmed by measurements of crystallographic orientation using EBSD (Figs. 4 and 5).

Most melt pseudomorphs from the Wet Mountains, and all of the melt pseudomorphs along subgrain boundaries in quartz and plagioclase, are now composed of K-feldspar, locally rimmed by plagioclase. The metapelitic rocks do not contain significant amounts of plagioclase; thus none of the plagioclase grains contain former melt on their subgrain boundaries. Granitic gneisses preserve melt pseudomorphs along subgrain boundaries in quartz and plagioclase in relatively equal amounts. Many more melt pseudomorphs in the gneisses are present along grain boundaries than subgrain boundaries; the amount of former melt located along subgrain boundaries is likely less than 5% of the total former melt in these rocks.

Textures due to former melt along subgrain boundaries in quartz grains from metapelitic rocks extend partway to fully along each subgrain boundary (Fig. 4A–C) and are commonly laterally continuous with melt pseudomorphs present along the grain boundaries (Fig. 4B and C). This continuity provides strong evidence that the material present along the subgrain boundaries represents former melt. The blebs of former melt are either pointed or rounded at the tip with an overall cuspate shape and have variable thickness, from 20 to 200 μm along their lengths (Fig. 4A–C). In Fig. 4A the former melt is not continuous with inferred former melt along grain boundaries, but the uniform blue color of the K-feldspar throughout the photomicrograph suggests these similarly-oriented grains are connected in the third dimension. Grains of sillimanite present within some of the melt pseudomorphs found along subgrain boundaries (Fig. 4B) are interpreted to have coarsened in the presence of melt due to enhanced diffusion. Fig. 4C shows an example in which melting occurred all the way along the subgrain boundary, resulting in two separate quartz grains with melt pseudomorphs along their boundary. The low angle grain boundary now visible is inferred to represent a former subgrain boundary.

Former melt along subgrain boundaries in quartz from granitic gneisses has a different morphology from that in the metapelites (Fig. 4D). In the gneisses, melt pseudomorphs at subgrain boundaries are much thinner (10—30 μm in width) and extend only a short distance into the grain, with minor variations in thickness along their width (Fig. 4D). Within plagioclase grains the former melt also does not extend very far into the crystal; it may be discontinuous and it is very thin, commonly less than 10 μm in width, with an angular morphology and pointed tips (Fig. 4E). Many melt pseudomorphs along subgrain boundaries in these granitic gneisses are interconnected and optically continuous with former melt along the grain boundaries.

EBSD misorientation data for the area within the yellow box, labeled Fig. 5 from Fig. 4A, follows the same procedures outlined for Figs. 2 and 3. Two profiles are shown on the misorientation map (Fig. 5A), one of which does not cross the former melt film. The orange transect is perpendicular to the tip of a former melt film (Fig. 5A) and based on the photomicrograph (Fig. 4A) may represent the character of the grain before partial melting occurred. Both subgrain boundaries and Dauphiné twins occur along the orange transect, with subgrain boundary misorientations ranging from 1 to 5° (Fig. 5A and B). Within the Dauphiné twin that extends from 60 to 110 μm along the orange transect, there are two subgrain boundaries, one of which has a misorientation of 4° (located at a distance of approximately 90 μm along the transect), and which connects to and is in the same orientation as the tip of the former melt (Fig. 5A and B). The green transect crosses the former melt film and displays multiple Dauphiné twins, including a twin boundary that runs along and parallel to the former melt film (Fig. 5A and B). Pole figures (Fig. 5C) on either side of the former melt film (red and blue boxes in Fig. 5A) show a rotation around {r}, consistent with activity of the slip system {π′} <a> (Lloyd et al., 1997; Lloyd, 2004). Misorientation data from the cyan box (Fig. 5A), shown on an inverse pole figure also plots near {r}, supporting the interpretation of activity on the slip system {π′} <a> (Fig. 5D). Additionally the inverse pole figure also suggests rotations around {π′}, and {a}, consistent with activity of the {r}<a>, and {m}<c> slip systems, respectively. Thus in this location, former melt is associated with subgrains formed by several different slip systems, indicating it was a high strain area. The association with Dauphiné twins further supports a stress-induced mechanism for Dauphiné twin formation.

Former melt on grain boundaries of all Wet Mountains rocks is morphologically similar to melt pseudomorphs along subgrain
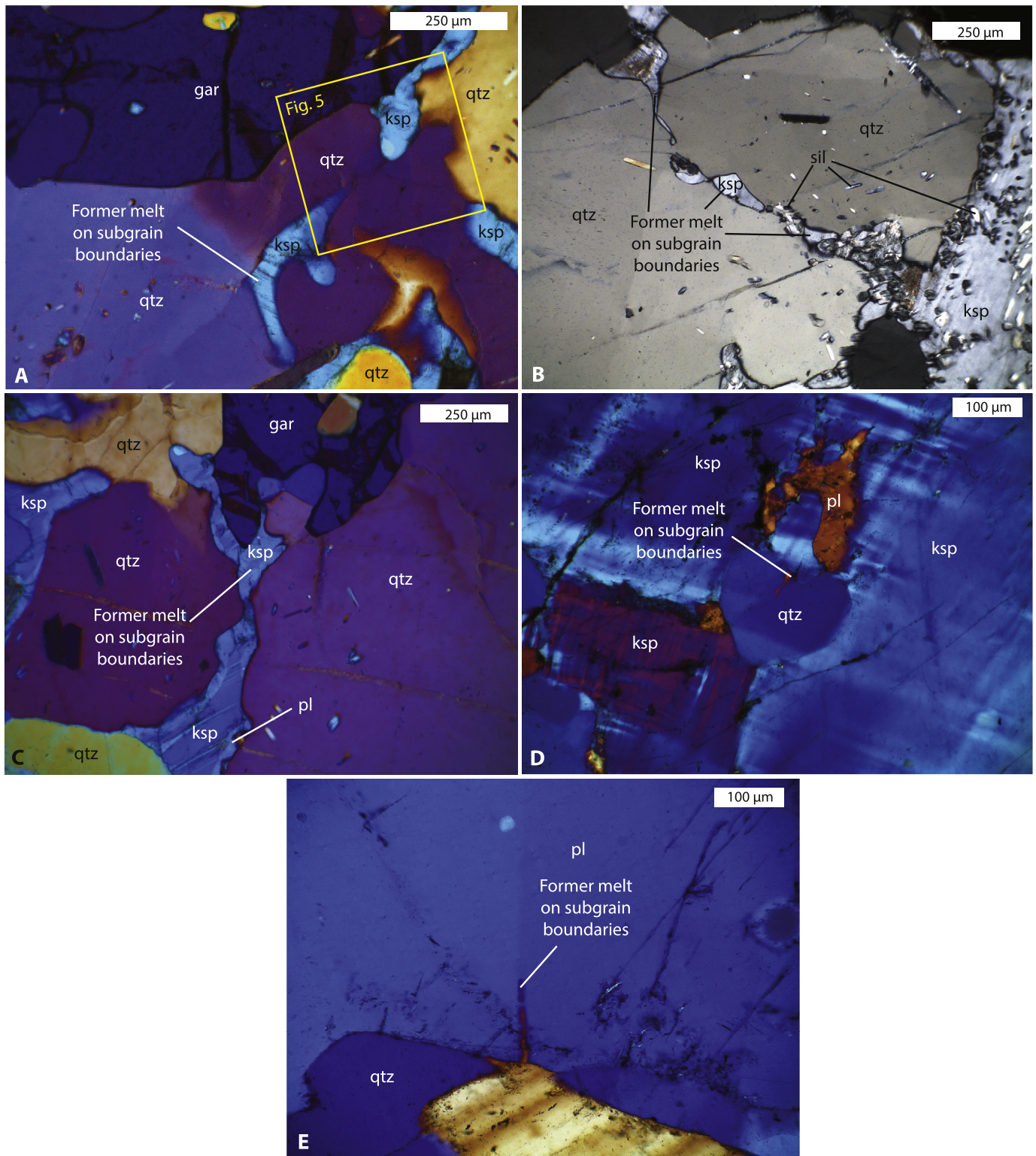
Fig. 4. Photomicrographs of former melt along subgrain boundaries in rocks from the Wet Mountains, central Colorado. All images in crossed polars; all but B with gypsum plate. A. Former melt, now K-feldspar (blue) along subgrain boundary in quartz (blue/purple). This former melt is not quite continuous with former melt along the grain boundary between quartz and biotite or quartz and garnet, but has the same optic orientation. Former melt is up to 100 μm in width and has pointed tips along the subgrain boundary. Yellow box marked Fig. 5 is the location of an EBSD misorientation map shown in Fig. 5. B. Former melt, now K-feldspar, with inclusions of sillimanite, along subgrain boundary in quartz. Former melt is nearly continuous along the subgrain boundary and ranges from 10 to 75 μm in width. C. Former melt, now K-feldspar with plagioclase rims (blue) along a subgrain boundary in quartz. This melt pseudomorph extends all the way across the subgrain boundary, and there are now two grains of quartz separated by the former melt. D. Former melt (orange) along subgrain boundary in quartz (blue). Former melt is very thin, less than 10 μm in width, is only present at the interface between the grain and subgrain boundary, and does not extend very far into the quartz crystal. E. Former melt, now K-feldspar (orange) along subgrain boundary in plagioclase (blue) and along quartz/plagioclase grain boundary. This melt pseudomorph is only present at the edge of the subgrain boundary, is less than 10 μm in width, and is discontinuous. qtz = quartz, ksp = K-feldspar, pl = plagioclase, gar = garnet, and sil = sillimanite.
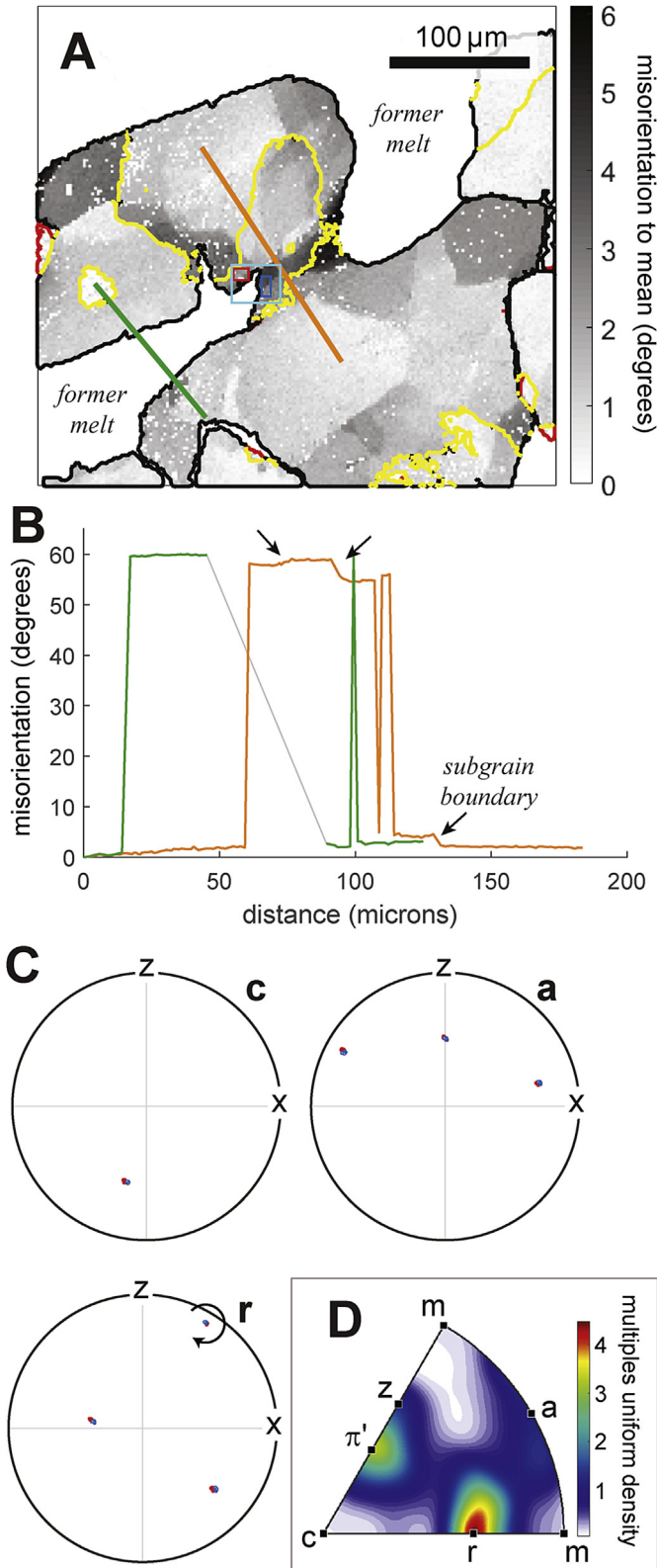
Fig. 5. Quartz EBSD data for area shown in Fig. 4A; plotting conventions are the same as those in Fig. 2. A. Misorientation map, showing a finger of former melt parallel to subgrain boundaries. B. Misorientation transects that illustrate both subgrain boundaries and Dauphiné twins near the former melt bleb. C. Pole figures of pixels from either side of the subgrain boundary near the tip of the former melt, suggesting a small misorientation around {r}. D. Misorientation axes for misorientations between 2 and 10° from the cyan region near the tip of the former melt, suggesting rotations around

boundaries. Melt pseudomorphs along grain boundaries in granitic gneisses are not typically more than 50 μm in width and have very little variation in thickness along their length. In the metapelitic rocks some melt pseudomorphs are laterally continuous over several centimeters, and these are interpreted to be former melt channelways (see Levine et al., 2013). Former melt along grain boundaries and subgrain boundaries is less abundant in the gneisses than in the metapelitic rocks.

5.3. Albany-Fraser belt, southwestern Australia

Rocks of the Albany-Fraser Orogen provide evidence for partial melting during deformation, with leucocratic material associated with all structures, including foliations, fold hinges, necks of boudins, shear bands, and melt channels. Melt pseudomorphs are interpreted on the basis of serrate/cuspate grain boundaries between unlike phases and in areas where skeletal or corroded grains of biotite or amphibole are present. In these rocks, melt pseudomorphs are preserved as quartz, plagioclase, or K-feldspar, but most commonly they consist of quartz or K-feldspar, likely because these rocks are plagioclase-rich. Former melt is found in roughly equal proportions along subgrain boundaries in both plagioclase and quartz.

Former melt preserved along subgrain boundaries in both plagioclase and quartz grains is typically found along the grain boundaries, with short segments of former melt along subgrain boundaries (Fig. 6). Melt pseudomorphs in both quartz and plagioclase are very thin, not more than 20–30 μm in width, and are commonly laterally and optically continuous with former melt along grain boundaries (Fig. 6). Melt pseudomorphs typically have pointed or square tips, a cuspate shape, and they have almost no lateral changes in thickness.

Most of the former melt in samples from the Albany-Fraser Belt is found along grain boundaries and has the same thin (20–60 μm wide) morphology as seen along subgrain boundaries. Melt pseudomorphs along grain boundaries commonly have pointed tips, minor lateral changes in thickness and are not localized at triple junctions. Pseudomorphs of melt along subgrain boundaries are rare in these rocks in comparison with occurrences of former melt along subgrain boundaries in the other two locations. Many of the melt pseudomorphs on subgrain boundaries appear to represent incipient melting in these locations, potentially representing a snapshot of the initiation of melting along subgrain boundaries.

5.4. Summary of observations and comparison of the areas

Rocks from three different field areas have experienced partial melting, via a variety of different reactions. All preserve former melt along subgrain boundaries in plagioclase and quartz. Lengths and widths of former melt along subgrain boundaries vary with location and the type of mineral containing the melt pseudomorph. None of the samples have former melt present along subgrain boundaries in K-feldspar, in part because very few grains of K-feldspar contained optical subgrains. Moreover, K-feldspar is less abundant than quartz or plagioclase in all three areas, so there are fewer locations for the K-feldspar component of the melt to nucleate.

Granitic gneisses from both the Lost Creek Gneiss and the Wet Mountains provide evidence for granitic wet melting reactions. Within these granitic gneisses former melt at grain boundaries is morphologically similar to the former melt microstructures along

---

{r}, {π'}, and {a}, consistent with activity of the {π'}<a>, {r}<a>, and {m}<c> slip systems, respectively.
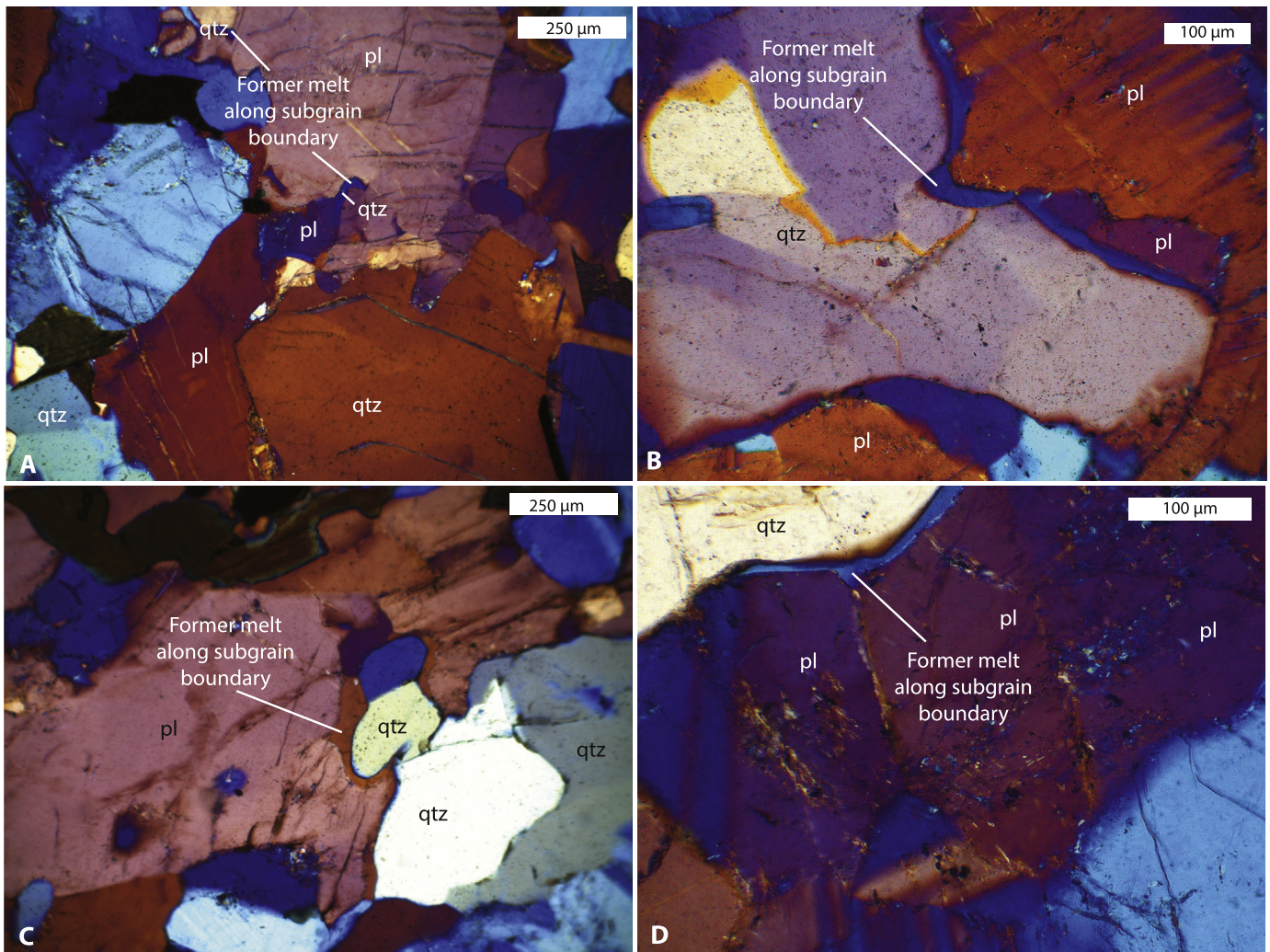
Fig. 6. Photomicrographs of melt pseudomorphs along subgrain boundaries in rocks from the Albany-Fraser Belt, southwestern Australia. All photomicrographs are in crossed polars with the gypsum plate inserted. A. Plagioclase grain shown in pink, in the top center of the image, with two subgrain boundaries containing former melt, now quartz, blue in color. Both of these melt pseudomorphs are quite thin, only 20–30 μm in width, and are also present at the edge of the plagioclase grains, on the plagioclase-quartz boundary. B. Former melt (blue), now K-feldspar, along a grain boundary between quartz and plagioclase. This former melt extends a very slight distance into the quartz grain along a subgrain boundary, and is very thin, only 30 μm in width. C. A melt pseudomorph, seen in orange in the center of the image, with a cuspate shape against a subgrain boundary in plagioclase (pink). This former melt is now composed of K-feldspar and is laterally continuous with former melt along the grain boundary between quartz and plagioclase. D. Former melt (blue), along a grain boundary between plagioclase and quartz. This melt pseudomorph is now K-feldspar, is 10 μm in width, and is also present along the subgrain boundary in plagioclase. qtz = quartz and pl = plagioclase.

subgrain boundaries. Overall there are fewer melt pseudomorphs in rocks that experienced granitic wet melting than locations that experienced dehydration melting. This difference likely occurs because melt that formed would have preferentially crystallized onto abundant pre-existing grains of quartz or plagioclase. Thus, fewer melt pseudomorphs formed along grain boundaries and subgrain boundaries, but this does not reflect the volume of melt that originally formed.

Rocks from the Wet Mountains and the Albany-Fraser Belt experienced a variety of dehydration melting reactions, including: muscovite-, biotite-, and amphibole-dehydration melting. Albany-Fraser Belt samples with plagioclase grains hosting the former melt only contain melt pseudomorphs at subgrain and grain boundary intersections and, in these locations, they are less abundant, thinner, and shorter than in other samples. Samples from metapelitic rocks of the Wet Mountains provide abundant evidence for melting along subgrain boundaries, with examples of melting nearly or all the way across a quartz grain, and development of new

grains separated by a narrow channel of former melt. In these samples, former melt along subgrain boundaries has greater widths and lengths than those in the other rock types. These differences in pervasiveness of melt pseudomorphs along subgrain boundaries likely reflects the composition of the host rock which controls the likelihood of melt being able to nucleate on preexisting grains, and perhaps the overall degree of partial melting the rocks experienced.

6. Discussion

The presence of former melt along subgrain boundaries in quartz and plagioclase in rocks from three diverse field locations indicates that partial melting commonly occurs along subgrain boundaries in migmatitic terranes. Former melt along subgrain boundaries of deformed rocks has not been previously documented by other workers, but its presence indicates a link between the partial melting process and dislocations.

In migmatitic terranes, the presence of leucosome material

along foliation surfaces, axial planes of folds, in the necks of boudins, and shear zones has typically been interpreted as exploitation of pre-existing structures as melt conduits (Sawyer, 1994; Brown, 1994). This melt migration is generally attributed to stress or pressure gradients (Robin, 1979; Stevenson, 1989; Cooper, 1990; Sawyer, 1994; Collins and Sawyer, 1996; Marchildon and Brown, 2001; Mancktelow, 2002), buoyancy flow driven by gravity (McKenzie, 1984; Wolf and Wyllie, 1993), and volume change associated with melting reactions (Wickham, 1987; Beckerman and Viskanta, 1988; Davidson et al., 1994; Brown et al., 1995).

In the case of former melt found along subgrain boundaries, it is unlikely that melt could exploit these boundaries only as a pre-existing conduit. Subgrain boundaries are planar arrangements of dislocations within a crystal lattice and diffusion of atoms can occur preferentially in these areas by pipe diffusion. Melt, however, cannot migrate along the subgrain boundaries without disruption of the lattice through melting along this boundary. Volume changes associated with melting reactions may cause fracturing; thus, fractures could nucleate on pre-existing subgrain boundaries and allow injection of melt into these composite subgrains.

Several lines of evidence indicate that the observed former melt did not occur along fractures coincident with subgrains. All of the subgrain boundaries that contain former melt were visible in polarized light but not in plane polarized light, indicating that they are not fractures. None of the subgrains evaluated in this study are coincident with fluid inclusion planes, which are characteristic of healed fractures that are commonly identified optically by planes of fluid inclusions along the former crack (Tuttle, 1949; Shelton and Orville, 1980; Roedder, 1984; Smith and Evans, 1984). Results from experimental studies suggest it may be difficult to differentiate healed fractures from subgrains, because dislocations decorated with small bubbles surrounding and in contact with fluid inclusions were located within healed fractures (Bakker and Jansen, 1991, 1994; Vityk et al., 2000). However, in these experimental studies, some of the primary fluid inclusions remained in addition to the newly nucleated bubbles and dislocations (Bakker and Jansen, 1991, 1994; Vityk et al., 2000). Such fluid inclusions were not observed along the subgrain boundaries in this study. Furthermore, subgrain boundaries analyzed through EBSD commonly had rotations around the *a*-axis, indicative of high-temperature prism[c] slip (Mainprice et al., 1986; Okudaira et al., 1995).

All of the melting reactions that occurred in these rocks require multiple reactants to produce melt ± a peritectic phase. For the reactions to occur, all of these reactants must be present, and in close enough proximity to each other to allow the reaction to proceed. Therefore, melting along the subgrain boundary does not occur in isolation from the rest of the system. Melting of the host grain must occur synchronously with melting in the rest of the rock, most likely along the adjacent grain boundary. This requirement explains two observations from these rocks: 1) melt pseudomorphs along subgrain boundaries are commonly optically and laterally continuous with former melt along adjacent grain boundaries, and 2) the compositions of the former melt and the host grain differ. Former melt crystallizes as a monomineralic film, composed of the least abundant phase in a sample. In fact, if a host quartz grain melted along subgrain boundaries in isolation from the rest of the rock, the composition of the melt would have to be the same as the host. Thus the former melt would not be optically distinguishable from the host mineral, unless impurities were present or accumulated at the subgrain boundary.

The observation that former melt along subgrain and grain boundaries is commonly laterally continuous, and that it has a different composition than the host mineral, provides additional support for the interpretation that the material on the subgrain

boundaries is indeed a melt pseudomorph. These textural and morphological characteristics are similar to other melt microstructures interpreted to represent melt pseudomorphs (Harte et al., 1991; Sawyer, 1999, 2001; Rosenberg and Riller, 2000; Holness and Sawyer, 2008). All of these criteria combined together provide strong support for subgrain boundaries in quartz and plagioclase being preferentially consumed in partial melting reactions because they contain high dislocation densities. Melting preferentially of these highly strained minerals is a local phenomenon; the overall degree of strain in an outcrop or hand sample is unlikely to affect the degree of melting along a subgrain boundary. Only the presence or absence of a subgrain boundary and the dislocation density of that subgrain boundary is likely to affect whether melting occurs.

6.1. Mechanisms of strain-induced melting

The evidence we have presented here documents preferential partial melting along subgrain boundaries. This localized melting indicates that material along subgrain boundaries contributes to the partial melting reaction. Four possible ways that high dislocation densities could contribute to preferential melting along subgrain boundaries are: 1) activation energy required for partial melting is lower because of a contribution from stored strain energy (Hand and Dirks, 1992); 2) less energy is needed to melt in this location because of an increased abundance of weakened bonds along the subgrain boundary; 3) enhanced diffusion rates along the subgrain boundary occur because of pipe diffusion or interstitial hydrogen/hydroxyl groups preferentially located at dislocations (Smoluchowski, 1952; Luther, 1965; McLaren et al., 1983; Kronenberg et al., 1986, 1990; Yurimoto and Nagasawa, 1989; Piazolo et al., 2016); and 4) the melting temperature is locally lowered due to the presence of water, including hydrogen/hydroxyl groups located at dislocations, or rare fluid inclusions (Seaman et al., 2013). The first two cases are similar because both assume partial melting occurs preferentially in more highly-strained locations because less energy is needed for reaction, whereas the latter scenarios focus on the role of water and its presence in the mineral lattice in higher strain locations.

An energetic contribution to the reaction from the stored strain energy in dislocations has been proposed, and experiments indicate preferential localization of reaction into very highly strained minerals (Green, 1972). Green (1972) experimentally deformed flint, and more highly strained areas preferentially transformed to coesite at temperatures as low as 450 °C and pressures of 1.0 GPa, conditions below the coesite stability field. These lower temperature and pressure conditions at which coesite formed metastably were attributed to a contribution from stored strain energy of at least 1200–4100 J/mol, the difference in free energy of strain-free quartz and coesite. Subsequent studies suggest that naturally deformed rocks are unlikely to have dislocation densities higher than 10^9 cm^{-2}, which would contribute only ~3 J/mol (Knipe and White, 1979; Wintsch and Dunning, 1985), a negligible amount of energy unlikely to alter reaction rates. However, dislocation densities within dislocation tangles, pileups, and subgrain boundaries, can be as high as 10^{11} cm^{-2} (Wintsch and Dunning, 1985). At sites with dislocation densities this high, the energetic input from dislocations becomes significant, with values proposed to range from 100 to 600 J/mol for densities of 10^{11} cm^{-2} (Wintsch and Dunning, 1985; Liu et al., 1995). Although dislocation tangles and pileups may have higher dislocation densities than subgrain boundaries, they are not favorable sites for partial melting, because all of the reactants required for partial melting must be in contact with each other. Subgrain and grain boundaries are connected and communicating, whereas a dislocation tangle in the middle of a quartz

crystal is not connected to plagioclase and K-feldspar grains nearby.

Typical activation energies for diffusion in hydrous melts have been estimated at approximately 150–300 kJ/mol (Rubie and Brearley, 1990). Although activation energies for diffusion in melts are not the same as activation energies for a partial melting reaction, they may have approximately the same magnitude. Energy differences between stored strain energy and activation energy for diffusion are four orders of magnitude apart, suggesting stored strain energy most likely makes a minor but potentially important contribution.

Dislocations are areas where the crystal lattice is distorted and planes or half-planes of atoms are missing or added, or the lattice is twisted along screw dislocations, resulting in large numbers of stretched and weakened bonds. Areas of high dislocation density are therefore likely to have higher numbers of weakened bonds than the rest of a mineral's crystal lattice. The melting process involves the weakening of bonds and disruption of the crystal lattice, and consequently would require less additional thermal input to weaken the bonds in deformed areas with high numbers of weak bonds. It is difficult to quantify the effect of this mechanism in causing partial melting, but most likely it is important in conjunction with other factors.

Both of the above mechanisms may provide some energetic contribution to the partial melting reaction, but in a multicomponent system, eutectic melting involves communication between the phases undergoing melting and transport of the reactants from non-adjacent sites. Thus, the presence of former melt along subgrain boundaries requires that diffusion along subgrain boundaries has occurred.

The presence of water within quartz and other nominally-anhydrous minerals, associated with dislocations, could influence the partial melting process by enhancing diffusion rates, speeding up partial melting reactions, and/or by locally reducing the temperature of melting. TEM images of dislocations in quartz show water bubbles at the ends of dislocations and strings of water bubbles present along subgrain and grain boundaries (Christie and Ord, 1980; McLaren et al., 1983; Koch et al., 1989; Meng et al., 2009). These water bubbles have been interpreted to form initially as interstitial H^+ defects and have coalesced into bubbles during heating (McLaren et al., 1983). The amount of water present along subgrain boundaries is difficult to quantify and may be small, but some studies indicate dislocation cores may be saturated with water (Heggie and Jones, 1986; Heggie, 1992). Experimental studies on water content in quartz indicate a range of water quantities of 20–600 ppm by weight, with more deformed samples containing higher water contents (Kronenberg and Wolf, 1990; Stipp et al., 2006; Gleason and DeSisto, 2008). This water associated with dislocations will enhance diffusion through increased transport rates of reactants along subgrain boundaries, including the reactant water, allowing and enhancing melting along subgrain boundaries, which also are energetically susceptible to melting. Water associated with dislocation cores could reduce the melting temperature (Tuttle and Bowen, 1958; Luth et al., 1964; Holtz et al., 1992; Becker et al., 1998), and recent work by Seaman et al. (2013) has shown that the presence of water in fluid inclusions, and/or associated with dislocations could lower melting temperatures up to a couple of hundred degrees Celsius. Water has two main contributions: enhancing diffusion rates throughout crystals and along grain and subgrain boundaries, and providing a needed reactant in the partial melting reaction.

EBSD misorientation analysis from quartz grains in the Lost Creek Gneiss and the Wet Mountains shows that subgrain boundaries associated with former melt have larger misorientations than those unaffected by partial melting (Figs. 2, 3 and 5). Although there are many factors that may affect misorientation, larger

misorientations are associated with increasing strain and more abundant dislocations (Poirier and Nicolas, 1975; Pennock et al., 2005; Raimbourg et al., 2011). Additionally, the presence of more dislocations along subgrain boundaries with larger misorientations would also support an increase in water associated with dislocations and enhanced pipe diffusion along these boundaries.

Experiments on deformed quartzite have shown that the activation energy for diffusion varies depending on crystallographic orientation in quartz (Giletti and Yund, 1984; Farver and Yund, 1991; Mainprice and Jaoul, 2009, and references therein) and it is reduced with the addition of small quantities of water (Mainprice and Jaoul, 2009). The presence of water associated with dislocations in a subgrain boundary could contribute water to the melting reaction, enhance reaction rates, and locally lower the temperature required for melting, all leading to melting preferentially along subgrain boundaries. Additionally, once melting commences along grain boundaries and/or subgrain boundaries, melting of the more weakly bonded crystal along subgrain boundaries should occur preferentially over melting of the undeformed crystals, and the contribution from stored strain energy should further enhance melting. In summary, we suggest melting along subgrain boundaries should precede melting of the rest of the grains, due to a combination of the four factors we propose. However, an assessment of the relative contribution of each of these factors is beyond the scope of this work.

6.2. Initiation of melting along subgrain boundaries

The process of melting along subgrain boundaries likely begins with partial melting along triple junctions of reactant grains. For purposes of simplification, the partial melting process will be considered in a granitic gneiss, where melting occurs via the reaction,

Quartz + Plagioclase + K-feldspar + H_2O = Melt.
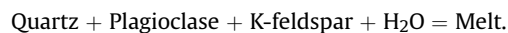
We provide a schematic diagram (Fig. 7) of partial melting which illustrates the timing of melting along subgrain boundaries relative to melting along grain boundaries and triple junctions, and can be compared to the actual photomicrographs from the different field areas.

Fig. 7A is a schematic diagram of a photomicrograph, in cross-polarized light, of deformed granitic gneiss with elongate quartz, one of which contains subgrains, and feldspar grains defining a foliation. Fig. 7A shows a triple junction where plagioclase, K-feldspar, and deformed quartz (+H_2O) are present, and is the location where melting typically occurs first, because the reactant grains are in contact (Mehnert et al., 1973). Melting will occur along many triple junctions in a rock as the melting temperature is reached, but for the purposes of this diagram, the process of melting will only be considered at one location (Fig. 7B).

Fig. 7 represents progressive time steps with an increasing degree of partial melting until crystallization (Fig. 7F). Fig. 7C shows melting at the triple junction and along grain boundaries where reactant grains and fluids are in contact. As melt forms along these boundaries, faster diffusion can occur within the melt and melting will proceed along grain boundaries, followed by subgrain boundaries. The melt/solid interfaces are cuspate because minerals are melting and their boundaries are becoming rounded (Mehnert et al., 1973). The highly strained quartz along the subgrain boundary is the source of quartz for this reaction (Fig. 7C) and can be compared to Figs. 4E and 6, with melting along subgrain boundaries only at the edge of the grain.

Continued melting leads to wetting of additional grain boundaries, progressive melting of reactant minerals, and continued
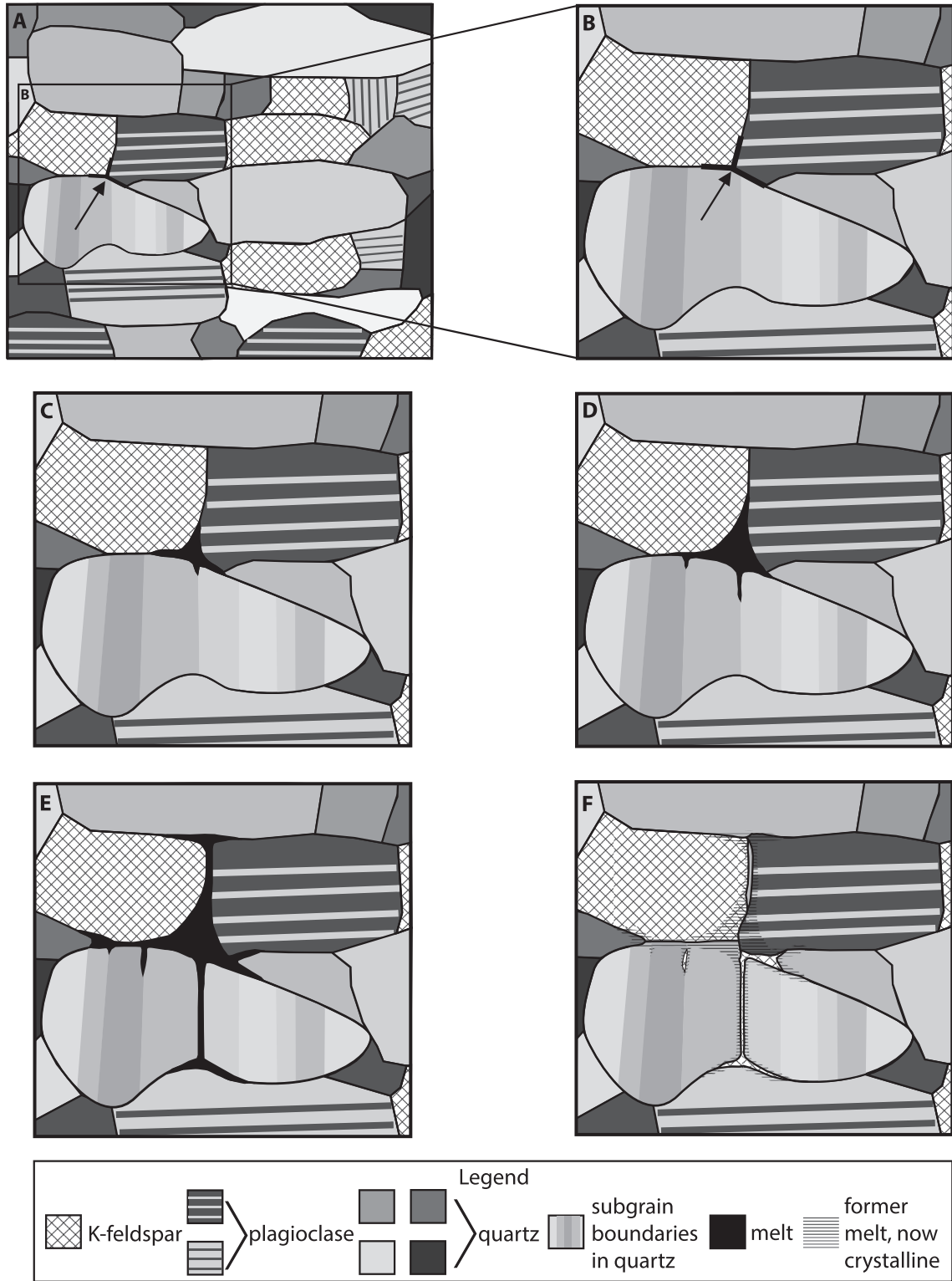
Fig. 7. Schematic diagram of a photomicrograph in crossed-polars, illustrating the model for partial melting along subgrain boundaries. Each image B—E represents a successive time-step in the partial melting process. See text for in depth description of figure. A. Deformed granitic gneiss with elongate quartz and feldspars, defining a foliation. The central left elongate quartz grain with the vertical bands of shading, represents a quartz grain with subgrains. The box in A is the area shown in B and all subsequent diagrams. B. A triple junction (highlighted in black, with an arrow) between deformed quartz, plagioclase and K-feldspar where melting could begin at sufficiently high temperature and pressure. C. Partial melting (melt shown in black) has begun at this triple junction, progressed along the grain boundary, and along the subgrain boundary in quartz. D. Partial melting has progressed along the triple junction, melt is now present further along the grain and subgrain boundaries and a second subgrain boundary, parallel to the first, has also started melting. E. Melting has progressed significantly and the deformed quartz grain has now been melted entirely through, forming two separate quartz grains. F. Crystallization. The former melt has nucleated and crystallized onto these pre-existing grains.

melting along the subgrain boundary and other parallel subgrain boundaries within the deformed quartz (Fig. 7D). Melting has progressed sufficiently for melt to transect the grain along the subgrain boundary, and Fig. 7E illustrates two quartz grains separated by a thin film of melt. Fig. 7E can be compared with Fig. 4C, where two quartz grains that appear to have a slight difference in orientation are separated by a thin film of former melt. Fig. 7F illustrates the preservation of this texture during crystallization of melt along subgrain boundaries, which are interconnected regions with grain boundaries. Shaded areas on the edge of mineral grains are locations that developed overgrowths due to nucleation and crystallization of the melt onto pre-existing grains. Melt pseudomorphs are preserved on grain and subgrain boundaries as quartz and K-feldspar; the pseudomorphs are preserved as these minerals because they are the modally least abundant phases. One subgrain melt pseudomorph is connected to a grain boundary pseudomorph, whereas the other one exists as an isolated film of K-feldspar.

Fig. 7 illustrates a subgrain boundary that is still connected, via the partial melt, to the other reactant phases that are melting. Consequently, eutectic melting can still occur, with the deformed quartz grain, K-feldspar, and plagioclase grains all continuing to melt. Melting will begin on grain boundaries and will progress to subgrain boundaries once melt has begun to form. Fig. 7D and E shows a number of the same features seen in Figs. 1, 4 and 6, illustrating that samples from the Lost Creek Gneiss, Wet Mountains, and Albany-Fraser Belt represent different degrees of partial melting along subgrain boundaries, with some incipient textures and several examples of complete or nearly complete melting across a subgrain boundary.

7. Conclusions

Melt pseudomorphs are found along subgrain boundaries in quartz and plagioclase from three field locations: the Lost Creek Gneiss of the Llano Uplift, central Texas, the Wet Mountains of central Colorado, and the Albany-Fraser Belt of southwestern Australia. The material found along subgrain boundaries is determined to be former melt on the basis of its textural and morphological similarity to former melt on grain boundaries and lateral and optically contiguity with melt pseudomorphs on grain boundaries. Consequently, former melt located along subgrain boundaries should be categorized as a new melt microstructure.

The presence of melt pseudomorphs along subgrain boundaries indicates that partial melting occurred preferentially in locations of high dislocation density. Melt pseudomorphs present along subgrain boundaries must have formed as a result of partial melting along subgrain boundaries; subgrain boundaries are not open conduits, and melt could not migrate into these locations without melting the host mineral. There are four factors that likely contribute to dislocations preferentially causing partial melting (no implied order of importance): 1) a lowering of the activation energy needed to cause reaction by contribution from stored strain energy, 2) an increased abundance of weakened bonds located within the subgrain boundary requiring less energy to weaken the remaining bonds, 3) enhanced diffusion rates along the subgrain boundary because of pipe diffusion or water bubbles located at dislocations, and 4) a local lowering of the melting temperature due to water associated with dislocations.

Acknowledgements

References

Alsayed, A.M., Islam, M.F., Zhang, J., Collings, P.J., Yodh, A.G., 2005. Premelting at defects within bulk colloidal crystals. Science 309, 1207–1210.

Bachmann, F., Hielscher, R., Schaeben, H., 2011. Grain detection from 2d and 3d EBSD data – specification of the MTEX algorithm. Ultramicroscopy 111, 1720–1733.

Bakker, R.J., Jansen, J.B.H., 1991. Experimental post-entrapment water loss from synthetic CO$_2$-H$_2$O inclusions in natural quartz. Geochimica Cosmochimica Acta 55, 2215–2230.

Bakker, R.J., Jansen, J.B.H., 1994. A mechanism for preferential H$_2$O leakage from fluid inclusions in quartz, based on TEM observations. Contrib. Mineral. Petrol. 116, 7–20.

Barbey, P., 2007. Diffusion-controlled biotite breakdown reaction textures at the solid/liquid transition in the continental crust. Contrib. Mineral. Petrol. 154, 707–716.

Becker, A., Holtz, F., Johannes, W., 1998. Liquidus temperatures and phase compositions in the system Qz-Ab-Or at 5 kbar and very low water activities. Contrib. Mineral. Petrol. 130, 213–224.

Beckerman, C., Viskanta, R., 1988. Natural convection solid/liquid phase change in porous media. Int. J. Heat Mass Transf. 31, 35–46.

Black, L.P., Harris, L.B., Delor, C.P., 1992. Reworking of Archaean and early Proterozoic components during a progressive, middle Proterozoic tectonothermal event in the Albany mobile Belt, western Australia. Precambrian Res. 59, 95–123.

Bodorkos, S., Clark, D.J., 2004. Evolution of a crustal-scale transpressive shear zone in the Albany-Fraser Orogen, SW Australia: 1. P-T conditions of Mesoproterozoic metamorphism in the Coramup Gneiss. J. Metamorph. Geol. 22, 691–711.

Brodie, K.H., Rutter, E.H., 1985. On the relationship between deformation and metamorphism with special reference to the behavior of basic rocks. In: Thompson, A.B., Rubie, D.C. (Eds.), Metamorphic Reactions: Kinetics, Textures, and Deformation. Springer, Berlin, pp. 138–179.

Brown, M., 1994. The generation, segregation, ascent and emplacement of granite magma: the migmatite-to-crustally-derived granite connection in thickened orogens. Earth Sci. Rev. 36, 83–130.

Brown, M., Averkin, Y., McLellan, E., Sawyer, E., 1995. Melt segregation in migmatites. J. Geophys. Res. 100, 15,655–15,679.

Carlson, W.D., Anderson, S.D., Mosher, S., Davidow, J.S., Crawford, W.D., Lane, E.D., 2007. High-pressure metamorphism in the Texas Grenville orogen: mesoproterozoic subduction of the southern Laurentian continental margin. Int. Geol. Rev. 49, 99–119.

Christie, J.M., Ord, A., 1980. Flow stress from microstructures of mylonites: example and current assessment. J. Geophys. Res. 85, 6253–6262.

Collins, W.J., Sawyer, E., 1996. Pervasive granitoid magma transfer through the lower-middle crust during non-coaxial compressional deformation. J. Metamorph. Geol. 14, 565–579.

Cooper, R.F., 1990. Differential stress induced melt migration: an experimental approach. J. Geophys. Res. 95, 6979–6992.

Dash, J.G., 1999. History of the search for continuous melting. Rev. Mod. Phys. 71, 1737–1743.

Davidson, C., Schmid, S.M., Hollister, L.S., 1994. Role of melt during deformation in the deep crust. TERRA Nova 6, 133–142.

Etheridge, M.A., Wall, V.J., Cox, S.F., Vernon, R.H., 1984. High fluid pressures during regional metamorphism and deformation: implications for mass transport and deformation mechanisms. J. Geophys. Res. 89, 4344–4358.

Farver, J.R., Yund, R.A., 1991. Oxygen fugacity in quartz: dependence on temperature and water fugacity. Chem. Geol. 90, 55–70.

Frondel, C., 1962. Dana's System of Mineralogy: III Silica Minerals. John Wiley and Sons, New York.

Giletti, B.J., Yund, R.A., 1984. Oxygen diffusion in quartz. J. Geophys. Res. 89, 4039–4046.

Gleason, G.C., DeSisto, S., 2008. A natural example of crystal-plastic deformation enhancing the incorporation of water into quartz. Tectonophysics 446, 16–30.

Green II, H.W., 1972. Metastable growth of coesite in highly strained quartz. J. Geophys. Res. 77, 2478–2482.

Green, H.W., Radcliffe, S.V., 1975. Fluid precipitates in rocks from the earth's mantle. Geol. Soc. Am. Bull. 86, 846–852.

Han, L., An, Q., Fu, R., Zheng, L., Luo, S., 2010. Local and bulk melting of Cu at grain boundaries. Phys. B 405, 748–753.

Hand, M., Dirks, P.H.G.M., 1992. The influence of deformation on the formation of axial-planar leucosomes and the segregation of small melt bodies within the migmatitic Napperby Gneiss, central Australia. J. Struct. Geol. 14, 591–604.

Harte, B., Pattison, D.R.M., Linklater, C.M., 1991. Field relations and petrography of partially melted pelitic and semi-pelitic rocks. In: Voll, G., Töpel, J., Pattison, D.R.M., Seifert, F. (Eds.), Equilibrium and Kinetics in Contact Metamorphism, the Ballachulish Igneous Complex and its Aureole. Springer-Verlag, Berlin and Heidelberg, pp. 182–210.

Heggie, M.I., 1992. A molecular water pump in quartz dislocations. Nature 355, 337–339.

Heggie, M.I., Jones, R., 1986. Models of hydrolytic weakening in quartz. Philos. Mag.

53, L65–L70.

Hielscher, R., Schaeben, H., 2008. A novel pole figure inversion method specification of the MTEX algorithm. J. Appl. Crystallogr. 41, 1024–1037.

Holness, M.B., Isherwood, C., 2003. The Aureole of the Rum Tertiary Igneous Complex, Inner Hebrides, Scotland. Journal of the Geological Society, London 160, pp. 15–27.

Holness, M.B., Sawyer, E.W., 2008. On the pseudomorphing of melt-filled pores during the crystallization of migmatites. J. Petrol. 49, 1343–1363.

Holness, M.B., Cesare, B., Sawyer, E.W., 2011. Melted rocks under the microscope: microstructures and their interpretation. Elements 7, 247–252.

Holtz, F., Pichavant, M., Barbey, P., Johannes, W., 1992. Effects of H$_2$O on liquidus phase relations in the haplogranite system at 2 and 5 kbar. Am. Mineral. 77, 1223–1241.

Humphreys, F., Huang, Y., Brough, I., Harris, C., 1999. Electron backscatter diffraction of grain and subgrain structures — resolution considerations. J. Microsc. 195, 212–216.

Kerrich, R., Fyfe, W.S., Gorman, B.E., Allison, I., 1977. Local modification of rock chemistry by deformation. Contrib. Mineral. Petrol. 65, 183–190.

Knipe, R.J., White, S.H., 1979. Deformation in low grade shear zones in the old red sandstone, S. W. Wales. J. Struct. Geol. 1, 53–66.

Koch, P.S., Christie, J.M., Ord, A., George Jr., R.P., 1989. Effect of water on the rheology of experimentally deformed quartzite. J. Geophys. Res. 94, 13,975–13,996.

Kronenberg, A.K., Wolf, G.H., 1990. Fourier transform infrared spectroscopy determinations of intragranular water content in quartz-bearing rocks: implications for hydrolytic weakening in the laboratory and within the earth. Tectonophysics 172, 255–271.

Kronenberg, A.K., Kirby, S.H., Aines, R.D., Rossman, G.R., 1986. Solubility and diffusional uptake of hydrogen in quartz at high water pressures: implications for hydrolytic weakening. J. Geophys. Res. 91, 12,723–12,744.

Kronenberg, A.K., Segall, P., Wolf, G.H., 1990. Hydrolitic weakening and penetrative deformation within a natural shear zone. In: Duba, A.G., Durham, W.B., Handin, J.W., Wang, H.F. (Eds.), The Brittle-ductile Transition in Rocks: the Heard Volume, American Geophysical Union Monograph, 56, pp. 21–36.

Kruhl, J.H., 1996. Prism- and basal-plane parallel subgrain boundaries in quartz: a microstructural geothermobarometer. J. Metamorph. Geol. 14, 581–589.

Kruhl, J., 1998. Reply: prism-and-basal-plane parallel subgrain boundaries in quartz: a microstructural geothermobarometer. J. Metamorph. Petrol. 16, 142–146.

Kuhlmann-Wilsdorf, D., 1965. Theory of melting. Phys. Rev. 140, A1599–A1610.

Levine, J.S.F., 2011. Investigation of the Role of Strain Localization in Preferentially Inducing Melting and the Criteria Used to Identify Anatectic Migmatites. PhD thesis. University of Texas at Austin.

Levine, J.S.F., Mosher, S., 2010. Contrasting Grenville-aged tectonic histories across the Llano Uplift, Texas: new evidence for deep-seated high-temperature deformation in the western uplift. Lithosphere 2, 399–410.

Levine, J.S.F., Mosher, S., Siddoway, C.S., 2013. Relationship between syndeformational partial melting and crustal-scale magmatism and tectonism across the Wet Mountains, central Colorado. Lithosphere 5, 456–476.

Liu, M., Yund, R.A., Tullis, J., Topor, L., Navrotsky, A., 1995. Energy associated with dislocations: a calorimetric study using synthetic quartz. Phys. Chem. Miner. 22, 67–73.

Lloyd, G.E., 2004. Microstructural evolution in a mylonitic quartz simple shear zone: the significant roles of dauphine twinning and misorientation. In: Alsop, G.I., Holdsworth, R.E., McCaffrey, K.J.W., Hand, M. (Eds.), Flow Processes in Faults and Shear Zones, 224. Geological Society, London, pp. 39–61. Special Publications.

Lloyd, G.E., Farmer, A.B., Mainprice, D., 1997. Misorientation analysis and the formation and orientation of subgrain and grain boundaries. Tectonophysics 279, 55–78.

Luth, W.C., Jahns, R.H., Tuttle, O.F., 1964. The granite system at pressures of 4 to 10 kilobars. J. Geophys. Res. 69, 759–773.

Luther, L.C., 1965. Diffusion along dislocations. J. Chem. Phys. 43, 2213–2218.

Lutsko, J.F., Wolf, D., Phillpot, S.R., Yip, S., 1989. Molecular-dynamics study of lattice-defect-nucleated melting in metals using an embedded-atom-method potential. Phys. Rev. B 40, 2841–2855.

Mainprice, D., Jaoul, O., 2009. A transmission electron microscopy study of experimentally deformed quartzite with different degrees of doping. Phys. Earth Planet. Inter. 172, 55–66.

Mainprice, D., Bouchez, J.L., Blumenfeld, P., Tubià, J.M., 1986. Dominant *c* slip in naturally deformed quartz: implications for dramatic plastic softening at high temperature. Geology 14, 819–822.

Mainprice, D., Lloyd, G.E., Casey, M., 1993. Individual orientation measurements in quartz polycrystals: advantages and limitations for texture and petrophysical property determinations. J. Struct. Geol. 15, 1169–1187.

Mancktelow, N.S., 2002. Finite-element modeling of shear zone development in viscoelastic materials and its implications for localization of partial melting. J. Struct. Geol. 24, 1045–1053.

Marchildon, N., Brown, M., 2001. Melt segregation in late syn-tectonic anatectic migmatites: an example from the Onawa Contact Aureole, Maine. USA. Phys. Chem. Earth (A) 26, 225–229.

McKenzie, D.P., 1984. The generation and compaction of partially molten rock. J. Petrol. 25, 713–765.

McLaren, A., Turner, R., Boland, J., Hobbs, B., 1970. Dislocation structure of the deformation lamellae in synthetic quartz; a study by electron and optical microscopy. Contrib. Mineral. Petrol. 29, 104–115.

McLaren, A.C., Cook, R.F., Hyde, S.T., Tobin, R.C., 1983. The mechanisms of the formation and growth of water bubbles and associated dislocation loops in synthetic quartz. Phys. Chem. Miner. 9, 79–94.

Mehnert, K.R., Büsch, W., Scheider, G., 1973. Initial melting at grain boundaries of quartz and feldspar in gneisses and granulites. Neues Jahrb. Fur Mineral. Monatsch. 4, 165–183.

Mei, Q.S., Lu, K., 2007. Melting and superheating of crystalline solids. From bulk to nanocrystals. Prog. Mater. Sci. 52, 1175–1262.

Meng, D., Wu, X., Fan, X., Meng, X., Zheng, J., Mason, R., 2009. Submicron-sized fluid inclusions and distribution of hydrous components in jadeite, quartz and symplectite-forming minerals from UHP hadeite-quartzite in the Dabit Mountains, China: TEM and FTIR investigation. Appl. Geochem. 24, 517–526.

Menegon, L., Piazolo, S., Pennacchioni, G., 2011. The effect of Dauphiné twinning on plastic strain in quartz. Contrib. Mineral. Petrol. 161, 635–652.

Misra, S., Burlini, L., Burg, J.-P., 2009. Strain localization and melt segregation in deforming metapelites. Phys. Earth Planet. Inter. 177, 173–179.

Mizushima, S., 1960. Dislocation model of liquid structure. J. Phys. Soc. Jpn. 15, 70–77.

Morgan, S.S., Law, R.D., 2004. Unusual transition in quartzite dislocation creep regimes and crystal slip systems in the aureole of the Eureka valley-Joshua flat-beer creek pluton, California: a case for anhydrous conditions created by decarbonation reactions. Tectonophysics 384, 209–231.

Mott, N.F., 1952. Introductory remarks. Proc. R. Soc. Lond. Ser. A, Math. Phys. Sci. 215, 1–4.

Neumann, B., 2000. Texture development of recrystallised quartz polycrystals unraveled by orientation and misorientation characteristics. J. Struct. Geol. 22, 1695–1711.

Nord, G.L., 1994. Transformation-induced twin boundaries in minerals. Phase Transit. 48, 107–134.

Okudaira, T., Takeshita, T., Hara, I., Ando, J-i, 1995. A new estimate of the conditions for transition from basal <a> to prism [c] slip in naturally deformed quartz. Tectonophysics 250, 31–46.

Ookawa, A., 1960. A model theory of liquid. J. Phys. Soc. Jpn. 15, 2191–2197.

Pehl, J., Wenk, H.-R., 2005. Evidence for regional Dauphiné twinning in quartz from the Santa Rosa mylonite zone in Southern California. A neutron diffraction study. J. Struct. Geol. 27, 1741–1749.

Pennock, G.M., Drury, M.R., 2005. Low-angle subgrain misorientations in deformed NaCl. J. Microsc. 217, 130–137.

Pennock, G.M., Drury, M.R., Spiers, C.J., 2005. The development of subgrain misorientations with strain in dry synthetic NaCl measured using EBSD. J. Struct. Geol. 27, 2159–2170.

Piazolo, S., Prior, D.J., Holness, M.D., 2005. The use of combined cathodoluminescence and EBSD analysis: a case study investigating grain boundary migration mechanisms in quartz. J. Microsc. 217, 152–161.

Piazolo, S., La Fontaine, A., Trimby, P., Harley, S., Yang, L., Armstrong, R., Cairney, J.M., 2016. Deformation-induced trace element redistribution in zircon revealed using atom probe tomography. Nat. Commun. 7, 10490. http://dx.doi.org/10.1038/ncomms10490.

Pluis, B., Denier van der Gon, A.W., Frenken, J.W.M., van der Veen, J.F., 1987. Crystal-face dependence of surface melting. Phys. Rev. Lett. 59, 2678–2681.

Poirier, J.P., 1985. Creep of Crystals. Cambridge University Press, Cambridge.

Poirier, J.P., Nicolas, A., 1975. Deformation-induced recrystallization due to progressive misorientation of subgrains, with special reference to mantle peridotites. J. Geol. 83, 707–720.

Prior, D., 1999. Problems in determining the misorientation axes, for small angular misorientations, using electron backscatter diffraction in the SEM. J. Microsc. 195, 217–225.

Prior, D.J., Boyle, A.P., Brenker, F., Cheadle, M.J., Day, A., Lopez, G., Peruzzo, L., Potts, G.J., Reddy, S.M., Spiess, R., Timms, N.O., Trimby, P.W., Wheeler, J., Zetterstrom, L., 1999. The application of electron backscatter diffraction and orientation contrast imaging in the SEM to textural problems in rocks. Am. Mineral. 84, 1741–1759.

Raimbourg, H., Kogure, T., Toyoshima, T., 2011. Crystal bending, subgrain boundary development, and recrystallization in orthopyroxene during granulite-facies deformation. Contrib. Mineral. Petrol. 162, 1093–1111.

Robin, P.-Y.F., 1979. Theory of metamorphic segregation and related processes. Geochimica Cosmochimica Acta 43, 1587–1600.

Roedder, E., 1984. Fluid inclusions. Mineral. Soc. Am. Rev. Mineral. 12, 70–77.

Rosenberg, C.L., Riller, U., 2000. Partial-melt topology in statistically and dynamically recrystallized granite. Geology 28, 7–10.

Rubie, D.C., Brearley, A.J., 1990. A model for rates of disequilibrium melting during metamorphism. In: Ashworth, J.R., Brown, M. (Eds.), High Temperature Metamorphism and Crustal Anatexis. Unwin Hyman, London, pp. 57–86.

Sawyer, E.W., 1994. Melt segregation in the continental crust. Geology 22, 1019–1022.

Sawyer, E.W., 1999. Criteria for the recognition of partial melting. Phys. Chem. Earth A24, 269–279.

Sawyer, E.W., 2001. Melt segregation in the continental crust: distribution and movement of melt in anatectic rocks. J. Metamorph. Geol. 19, 291–309.

Seaman, S.J., Williams, M.L., Jercinovic, M.J., Koteas, G.C., Brown, L.B., 2013. Water in nominally-anhydrous minerals: implications for partial melting and strain localization in the crust. Geology 41, 1051–1054.

Shelton, K.L., Orville, P.M., 1980. Formation of synthetic fluid inclusions in natural quartz. Am. Mineral. 65, 1233–1236.

Siddoway, C.S., Givot, R.M., Bodle, C.D., Heizler, M.T., 2000. Dynamic versus

anorogenic setting for mesoproterozoic plutonism in the wet mountains, Colorado: does the interpretation depend on level of exposure? Rocky Mt. Geol. 35, 91–111.

Sirong, Y., Dongcheng, L., Kim, N., 2006. Microstructure evolution of SIMA processed Al2024. Mater. Sci. Eng. A420, 165–170.

Smith, D.L., Evans, B., 1984. Diffusional crack healing in quartz. J. Geophys. Res. 89, 4125–4135.

Smoluchowski, R., 1952. Theory of grain boundary diffusion. Phys. Rev. 87, 482–487.

Stevenson, D.J., 1989. Spontaneous small-scale melt segregation in partial melts undergoing deformation. Geophys. Res. Lett. 16, 1067–1070.

Stipp, M., Tullis, J., Behrens, H., 2006. Effect of water on the dislocation creep microstructure and flow stress of quartz and implications for the recrystallized grain size piezometer. J. Geophys. Res. 111, B04201. http://dx.doi.org/10.1029/2005JB003852.

Tartaglino, U., Tosatti, E., 2003. Strain effects at solid surfaces near the melting point. Surf. Sci. 532–535, 623–627.

Trépied, L., Doukhan, J., Pacquet, J., 1980. Subgrain boundaries in quartz theoretical analysis and microscopic observations. Phys. Chem. Miner. 5, 201–218.

Tullis, J., Tullis, T., 1972. Preferred orientation of quartz produced by mechanical dauphiné twinning: thermodynamics and axial experiments. In: Heard, H.C., Borg, I.Y., Carter, N.I., Raleigh, C.B. (Eds.), Flow and Fracture of Rocks, American Geophysical Union Monograph, 16, pp. 67–82.

Tumarkina, E., Misra, S., Burlini, L., Connolly, J.A.D., 2011. An experimental study of the role of shear deformation on partial melting of a synthetic metapelite. Tectonophysics 503, 92–99.

Tuttle, O.F., 1949. Structural petrology of planes of liquid inclusions. J. Geol. 57, 331–356.

Tuttle, O.F., Bowen, N.L., 1958. Origin of granite in the light of experimental studies in the system NaAlSi$_3$O$_8$-KAlSi$_3$O$_8$-SiO$_2$-H$_2$O. Geol. Soc. Am. Mem. 74.

Urai, J.L., Means, W.D., Lister, G.S., 1986. Dynamic recrystallization of minerals. In: Hobbs, B.E., Heard, H.C. (Eds.), Mineral and Rock Deformation: Laboratory Studies, Geophysical Monograph, 36, pp. 161–199.

Vityk, M.O., Bodnar, R.J., Doukhan, J.-C., 2000. Synthetic fluid inclusions, XV. TEM investigation of plastic flow associated with reequilibration of fluid inclusions in natural quartz. Contrib. Mineral. Petrol. 139, 285–297.

Waters, D.J., 2001. The significance of prograde and retrograde quartz-bearing intergrowth microstructures in partially melted granulite-facies rocks. Lithos 56, 97–110.

Wenk, H.-R., Barton, N., Bortolotti, M., Vogel, S.C., Voltolini, M., Lloyd, G.E., Gonzalez, G.B., 2009. Dauphiné twinning and texture memory in polycrystalline quartz. Part 3: texture memory during phase transformation. Phys. Chem. Miner. 36, 567–583.

White, S., 1975. Tectonic deformation and recrystallization of oligoclase. Contrib. Mineral. Petrol. 50, 287–304.

White, S.H., 1977. Geological significance of recovery and recrystallization processes in quartz. Tectonophysics 39, 143–170.

Wickham, S.M., 1987. The segregation and emplacement of granitic magmas. J. Geol. Soc. Lond. 144, 281–297.

Wintsch, R.P., 1975. Feldspathization as a result of deformation. Geol. Soc. Am. Bull. 86, 35–38.

Wintsch, R.P., Dunning, J., 1985. The effect of dislocation density on the aqueous solubility of quartz and some geologic implications: a theoretical approach. J. Geophys. Res. 90, 3649–3657.

Wolf, M.B., Wyllie, P.J., 1993. Garnet growth during amphibolite anatexis: implications of a garnetiferous restite. J. Geol. 101, 357–373.

Yund, R.A., Tullis, J., 1991. Compositional changes of minerals associated with dynamic recrystallization. Contrib. Mineral. Petrol. 108, 346–355.

Yurimoto, H., Nagasawa, H., 1989. The analysis of dislocation pipe radius for diffusion. Mineral. J. 14, 171–178.